Scripta Materialia 239 (2024) 115802

Contents lists available at ScienceDirect

Scripta Materialia

journal homepage: www.journals.elsevier.com/scripta-materialia

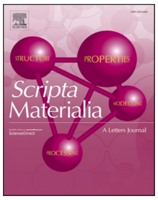

Observations of the occurrence and disappearance of peritectic couple growth performed under microgravity conditions

Andreas Ludwig [*], Johann Mogeritsch

Metallurgy Department, Montanuniversitaet Leoben, Franz-Josef Street 18, Leoben 8700, Austria

ARTICLE INFO

Keywords:
Peritectics
Couple growth
Transparent model alloy
Microgravity
Directional solidification

ABSTRACT

Peritectic couple growth (PCG) is an unusual growth form at which the peritectic and pro-peritectic solid phases solidify like a regular eutectic. To investigate the dynamics of PCG formation and growth, experiments with the transparent, organic peritectic alloy Tris(hydroxymethyl)aminomethane–Neopentylglycol are performed at the International Space Station. Fully planar and partly planar/cellular PCGs are found and analyzed. In any case, PCG starts with the formation of lateral bands from the peritectic phase that overgrow most of the pro-peritectic phase but not completely. During coupled growth, the remaining patches transform into rods and/or lamellae. Depending on the conditions, PCG either terminates by the disappearance of pro-peritectic rods or by transforming the rods into cells. The second mechanism goes hand in hand with the formation of a single-phase 2D layer at the top of a tilted interface. At low pulling velocities, planar pro-peritectic phase growth transforms into planar peritectic phase growth via PCG.

Many industrially relevant alloys, such as steels and other Fe-based alloys, Cu- and Ti-alloys, some magnetic materials and superconductor alloys [1] are peritectic alloys. If such alloys solidify with a low growth velocity such that a dendritic morphology is avoided, peritectic coupled growth (PCG) might occur, a growth form that resemble eutectic couple growth (ECG) [2,3]. Alloys with hypo-peritectic compositions can reach steady-state planar growth of the primary α-phase only with growth temperatures below the peritectic temperature. Therefore, a nucleation probability for the peritectic β-phase exists and thus, no stable conditions for planar growth of both solids might be found. For such alloys, an alternative growth of lateral bands of α and β was observed [4] and theoretically analyzed [5]. Herein, it was already mentioned that if the lateral growth rate is smaller than the growth rate of the parent phases, both phases may grow in a coupled manner and indeed PCG was also found experimentally [2,3,6–8]. It turned out that the occurrence of PCG depends on nucleation [9], diffusion length and container size [2,3,17,8,10–16] and convection ahead of the front [10,18–20].

In particular, the influence of convection on PCG created the need for experimental studies under purely diffusive conditions, in fact, experiments in microgravity (μg). As PCG occurs at slow growth velocities, corresponding long-lasting μg experiments could only be performed at the International Space Station (ISS). For *in-situ* observations of the dynamic of the PCG formation, the organic transparent peritectic model system tris(hydroxymethyl)aminomethane–neopentylglycol (TRIS–NPG) was selected. Between March 17 and April 24, 2021, three cartridges filled with TRIS-NPG alloys of near peritectic compositions were processed by using the 'TRANSPARENT ALLOY' (TA) insert to the MSG[1] [21–23]. It was shown that during the initial transient stage, the formation of PCG began with the occurrence of lateral bands of the peritectic β-phase in the gap between the pro-peritectic α-phase and cartridge glass window [23]. An inclined α/l interface enriched the solute at the backmost part of the solidifying interface, thus favoring the growth of β. A necessary condition that enables the β-phase band to reach the α/l interface is that the interface temperature should fall below T_p. The recoil of the s/l interface during the initial transient gradually reduces the interface temperature such that β can finally reach and overgrow the α/l interface. However, some larger α patches remain in contact with the liquid, and so, PCG begin. While the interface temperature further decrease, the α patches change into long lamellae, follow by an increasing number of curved lamellae with some rod-like objects. Finally, only rods grow coupled with the β matrix [23]. In the present letter, it is shown that fully planar PCG appears to be an intermediate stage during the initial transient that occurs when α changes into β planar solidification. In addition, it is shown that for larger pulling velocities, partly

---

* Corresponding author.
E-mail address: ludwig@unileoben.ac.at (A. Ludwig).

[1] Microgravity Science Glove-Box.

https://doi.org/10.1016/j.scriptamat.2023.115802
Received 15 May 2023; Received in revised form 27 September 2023; Accepted 1 October 2023
Available online 4 October 2023
1359-6462/© 2023 The Authors. Published by Elsevier Ltd on behalf of Acta Materialia Inc. This is an open access article under the CC BY license (http://creativecommons.org/licenses/by/4.0/).

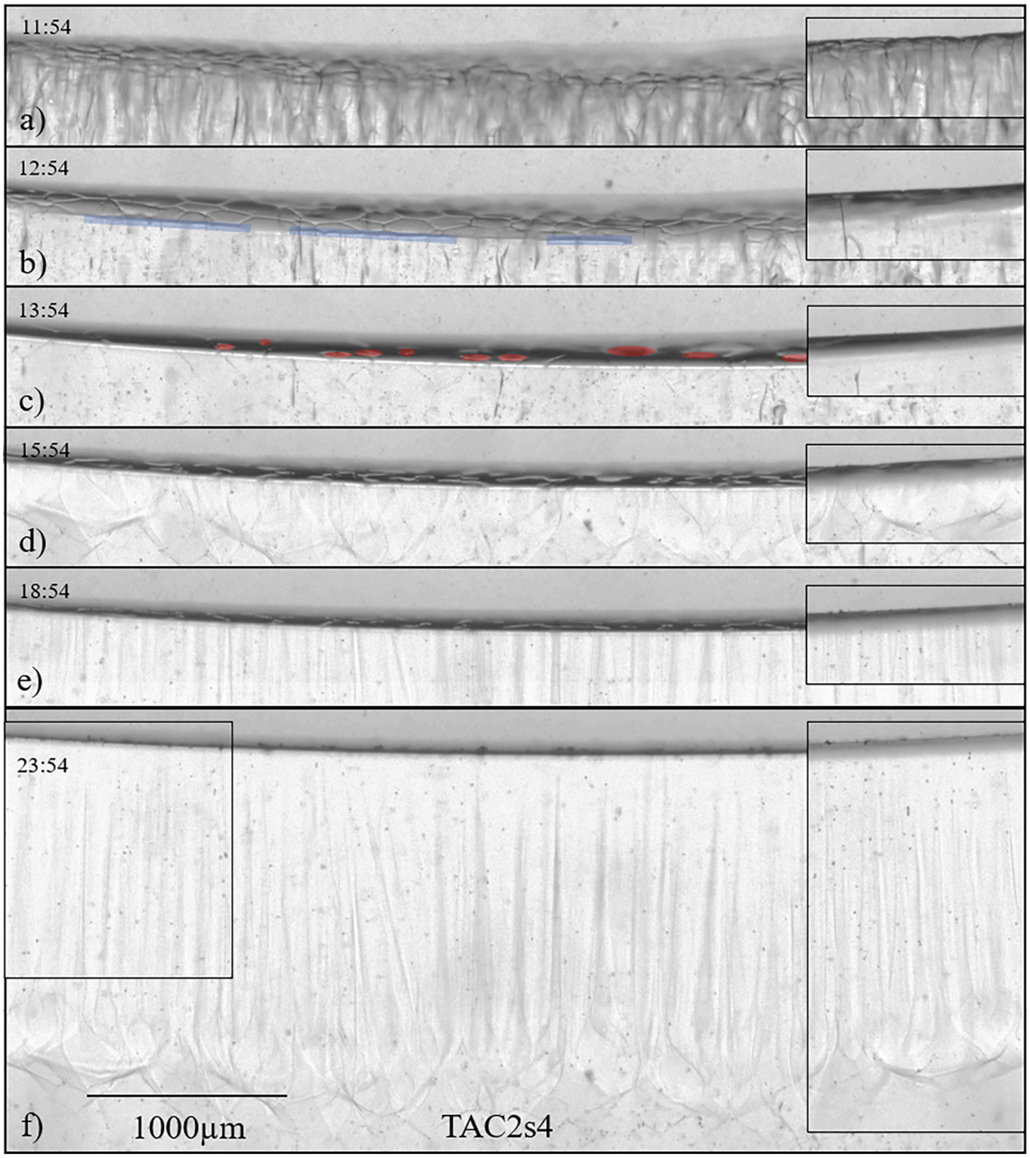

Fig. 1. Development and disappearance of PCG during solidification of segment TAC2s4 ($V_{\text{pull}} = 0.360$ mm/h). The growth direction is upwards. Pictures are taken with middle focus except the right insets, which are taken with front focus, and the left inset, which are taken with back focus. (a) is acquired at the ISS on April 8, 2021, 11:54 GMT, that's one hour after the start of the pulling, (b) to (f) is acquired later as indicated by the given clock time. The blue bars in (b) indicate the peritectic β-phase that approaches the growing α/l-interface. In (c) this interface is completely overgrown by the β-phase, except the α-patches that are (partly) indicated in red. These patches decrease in size until they completely disappear (f).

planar/cellular PCG coexists together with a single-phase 2D layer at the top of the tilted interface.

The TA apparatus used for the *in-situ* studies reported here was specifically designed for experiments with organic transparent alloys under μg-conditions [24]. Details concerning the performed experiments are presented in [23]. A schematic drawing of the Bridgman furnace and cartridge of the TA device can be found in [25]. The cartridges, named TAC, possessed a solidification volume of 100 mm (length) × 6 mm (width) × 1 mm (depth). Owing to specific requirements for the contact area between the cartridge and hot and cold clamps, only an effective solidification length of 66 mm was available. This length was conceptually separated into six segments (named S1-S6), with a length of 11 mm each. The solidification experiments were conducted one by one only with 'fresh' segments that had never melted before.

The two compounds' TRIS-NPG were supplied as powders by Sigma–Aldrich,[2] with a reported purity of >99.9% for TRIS and >99% for NPG. All manipulations with these compounds were performed under a protective atmosphere. The water content of NPG was further reduced by drying at 375 K for 24 h TRIS was used without further processing because it is sensitive to long-term annealing at elevated temperatures. Alloying and filling of special syringes were performed by the authors. The material was then shipped to QinetiQ Space,[3] where the TACs were filled.

A typical experiment started with 1 h sample annealing at elevated temperature (403 K, without visible traces of molten areas), then 2 h were added without any motion but with activating a predefined temperature gradient of $G \approx 3$–5 K/mm (gradient stage) and subsequently

---

[2] http://www.sigmaaldrich.com.

[3] https://www.qinetiq.com/en/sectors/space now https://redwirespace.com.

pulling was done with a constant velocity in the range of V_{pull} = 0.14–0.65 mm/h. Finally, the sample motion was stopped while the gradient was retained for another 4 h. In most cases, both hot clamps were set to $T_{\mathrm{hot}} = 439$ K and both cold clamps to $T_{\mathrm{cold}} = 379$ K.

After activating the temperature gradient, the organic material melted above the corresponding liquidus temperature and only partly below. The mushy zone that formed revealed a fine-grained microstructure. During the gradient stage, coarsening and grain boundary migration occurred by temperature gradient zone melting (TGZM) [26, 27], and thus the mush/liquid (m/l) interface recoiled. As a consequence, each solidification experiment started with a m/l interface that consisted of grains that were still much smaller than the spacing of the cartridge at a position that did not exactly represent the liquidus temperature of the corresponding alloy. Surprisingly, we observed in most of experiments, that the grains close to the front window were ahead of those close to the rear window. Thus, the m/l interface that served as the starting point for solidification was inclined. In addition, we realized that the m/l interface during the gradient stage and the s/l interface during growth were convexly curved seen from the ‘hot’ side of the field of view (FOV). It is important to mention that the amount of convexity is nearly constant during holding and growth. It is also almost symmetrical with respect to the cartridge axis.

Nine of the eighteen solidification experiments performed during the microgravity campaign showed PCG. We found both fully and partly planar/cellular PCG. Fig. 1 shows an example of a fully planar and Fig. 3 of partly planar/cellular PCG. Fully planar PCG was found for pulling velocities equal to or smaller than $V_{\mathrm{pull}} = 0.396$ mm/h and partly planar/cellular PCG for pulling velocities equal to or greater than $V_{\mathrm{pull}} = 0.360$ mm/h. The formation of PCG needed a minimal pulling velocity of $V_{\mathrm{pull}} = 0.324$ mm/h to occur. In contrast, an upper pulling velocity limit was not found, as actually for the largest applied pulling velocity, $V_{\mathrm{pull}} = 0.648$ mm/h, PCG was observed even if rapidly massive cellular growth occurs.

Fully planar PCG occurred when the s/l interface remained macroscopically planar. Some large-scale interface curvatures, such as the convexity in the width direction, did not cause morphological instability. The challenge of studying the formation of PCG with an organic transparent model system such as TRIS-NPG is that the pro-peritectic and peritectic phases look exactly the same, as they have similar refraction indices. The distinction can only be made by their different dynamical behaviors.

In Fig. 1b, peritectic phase bands (marked in blue) have reached the s/l interface from lower positions and started to grow over the interface from the back towards the front window. Although the optical illusion exists in that the bands in Fig. 1b are located at the front, they are definitely located at the rear window. This becomes clear as the inset at the right of the picture was taken with a focus at the front window at $ff_1 = 0$ mm, whereas the picture itself was taken with a focus in the middle between the front and rear windows at $ff_2 = 0.5$ mm.

The bands nearly overgrew the former interface except some patches that are marked in red in Fig. 1c. These patches changed into lamellae and finally into a mixture of lamellae and rods (Fig. 1c-f), while the front recoiled and thus gradually grew at lower interface temperatures. In the further course, the size of the lamellae and rods decreased until they finally completely disappeared. Thus, only a limited length solidifies with PCG. In the case of Fig. 1, the PCG region had an approximate length of 2 mm. Detailed investigations on the beginning and the end of PCG revealed that the solid phase that formed the bands is also the phase that finally prevails. As the primary existing grains comprised the pro-peritectic α-phase, the bands and the prevailing solid phase, comprised the peritectic β-phase. Therefore, Fig. 1 shows the transition from α to β growth via PCG. It is also worth mentioning that for TAC2s4, the recoil during PCG occurred with a nearly constant velocity of approximately $V = 0.180$ mm/h. That is 50% of the actual pulling velocity of $V_{\mathrm{pull}} = 0.360$ mm/h.

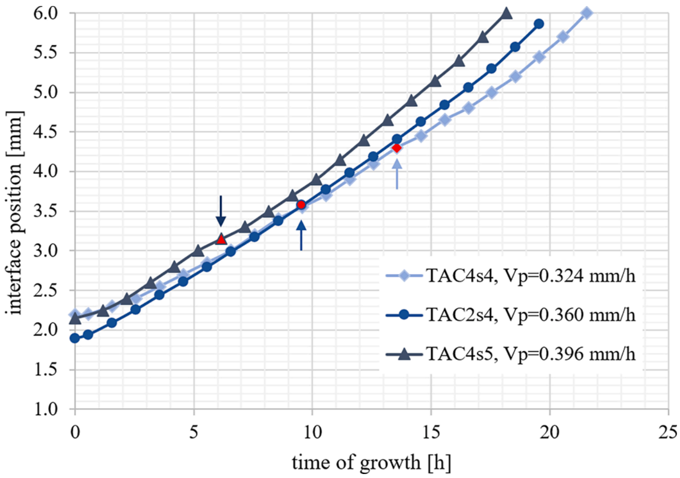

Fig. 2. Lowest interface position at the rear window as function of time. The time of growth are measured from the instant that the coagulated second phase band reaches the interface of the primary phase and thus the start of PCG. The termination of PCG is indicated by the red markers and the arrows.

Fig. 2 shows the central interface position at the rear window as a function of time for three different experiments that showed fully planar PCG. The beginning of the curves was taken at the start of the PCG. For TAC4s4, that was 3.9 h after the start of the pulling, and for TAC2s4 and TAC4s5, 2.4 h. The end of PCG is indicated by the arrows. The continuation of the interface recoil hereafter is based on the growth of only one single solid phase. Note that PCG occurred with similar growth velocities for TAC2s4 and TAC4s5, but TAC4s4 solidified with approximately $V = 0.200$ mm/h for the PCG stage (55% of V_{pull}).

Comparing the initial interface position with the (indirectly) estimated temperature profile along the cartridge axis and the TRIS-NPG phase diagram, reveals that TAC4s4 and TAC4s5 exhibited the same concentration, $c_0 = 51.5 \pm 1$ mol% NPG, whereas TAC2s4 exhibited $c_0 = 49.3 \pm 1$ mol% NPG. Therefore, all three segments most probably reveal a composition in the peritectic interval (47–54 mol% NPG), with TAC2s4 being hypo-peritectic and TAC4s4 and TAC4s5 hyperperitectic ($c_p = 51$ mol% NPG). This is surprising because hyperperitectic alloys should have fewer problems to form stable β-phase growth than hypo-peritectic alloys. On the other hand, due to the interface inclination, the solute concentration at the foremost and backmost part of the interface might be different. At the end of the PCG the interface recoiled by 3.1 mm for TAC4s5, 3.6 mm for TAC2s4 and 4.3 mm for TAC4s4. The corresponding PCG thickness can be directly linked to the pulling velocity. The lower the pulling velocity, the longer stable PCG can occur.

The prevailing phase at the end of PCG is the same that had formed the initial bands, obviously the peritectic β-phase. Comparing the interface temperature during further recoil with the phase diagram reveals that the β-phase solidified with an interface temperature that is below the melting point of pure NPG, which is obviously impossible. Thus, we have to assume that undesired impurities lowers the liquidus of the β-phase.

Partly planar/cellular PCG occurred for larger pulling rates. It was observed that the grains close to the front window started to grow faster and so soon grow ahead of the others. The inset of Fig. 3a, acquired two hours after the start of the pulling, shows that these grains grew as a thin solid layer with a two-dimensional rather than a three-dimensional characteristic. In the further course (Fig. 3b-e), they grew independent from the rest of the front and formed a clear distinct cellular pattern, while the rest of the front was still growing with planar PCG. As shown in Fig. 3b, PCG is again initiated by the formation of a coagulated second solid phase band (marked in blue) that appeared from deeper regions in the mush and grew from back to front after having reached the s/l interface. In Fig. 3c, the remaining patches of the primary solid phase are

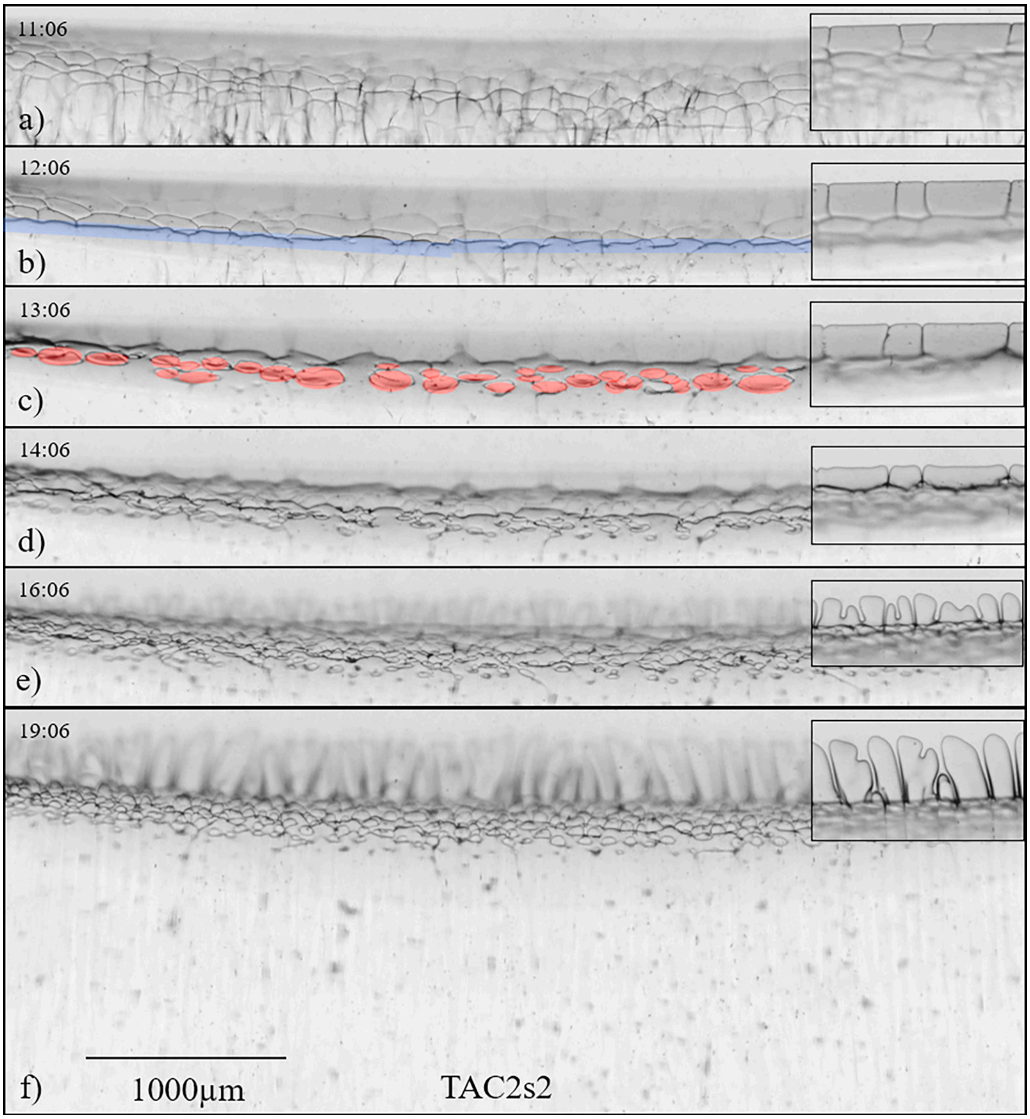

Fig. 3. Development of PCG during solidification of segment TAC2s2 ($V_{\text{pull}} = 0.432$ mm/h). The growth direction is upwards. Pictures are taken with middle focus except the insets, which are taken with front focus. (a) is acquired at the ISS on April 2, 2021, 11:06 GMT, that's 2 h after the start of the pulling, (b) to (f) are acquired later as indicated by the given clock time. Again, in (b) blue is used to indicate the peritectic β-phase that approaches the growing α/l-interface. In (c) this interface is overgrown by the β-phase, except a single-phase 2D layer at the top of the tilted interface and except the α-patches that are indicated in red.

again marked with red. Unlike the fully planar PCG, we have observed only rods that formed. They grew quite dynamically in competition with the second solid. Over time, the rods started to form cells, and the second phase was left behind (Fig. 3f). The cells further evolved, and finally, the whole interface became cellular or even dendritic (not shown). From the description given here, it is clear that the cells that have developed from the planar PCG front constitute the pro-peritectic α phase and that the matrix that is left behind constitutes the peritectic β phase. This was also confirmed by detailed studies on enlarged sections. Such cellular PCG was also observed by Dobler et al. [3]. They decreased the G/V_{pull} ratio beyond the limit of morphological stability of the pre-peritectic phase and got a transition from planar to cellular PCG. During our experiments, the interface recoil indicates that the system still passes through the initial transient stage where increasing solute pileup leads to a destabilization of the front and thus planar PCG changes into cellular PCG.

In Fig. 4, the interface position as a function of time for four experiments with partly planar/cellular PCG is given. Measured were the positions of the s/l interface tips at the front window together with the position of the roots of the thin solid layers. Different from Fig. 2, the beginning of the curves is now given by the start of pulling. The growth velocity of the thin solid layer was faster than the growth velocity of the left-behind interface. Therefore, for each experiment, we plotted a curve with two branches: one for the thin layer tip position (lower branch) and one for the left-behind bulk interface (upper branch). As mentioned above, the corresponding thin solid layer formed a polycrystalline interface that changed with time into a cellular pattern. The instant when this happens is marked with a yellow dot. The left-behind interface grew first as planar PCG and later as cellular PCG. However, as more and more distinctive cells occurred further evaluation of the interface position was no longer possible (end of the upper branch). It was also difficult to decide whether solidification continued as a cellular PCG with deep cells or as a single-phase cellular array. TAC2s1 became fully cellular after only 2 h. For all four experiments shown in Fig. 4, the start of the PCG (indicated by a red dot) occurred before the thin solid layer was established. For TAC2s2, we found a growth velocity of $V = 0.322$ mm/h for the initial polycrystalline growth and $V = 0.337$ mm/h for the cellular growth of the thin solid layer. These values are 75% and 78% of the pulling velocity of $V_{\text{pull}} = 0.432$ mm/h. PCG at the left-behind interface grew with only $V = 0.307$ mm/h so that the difference

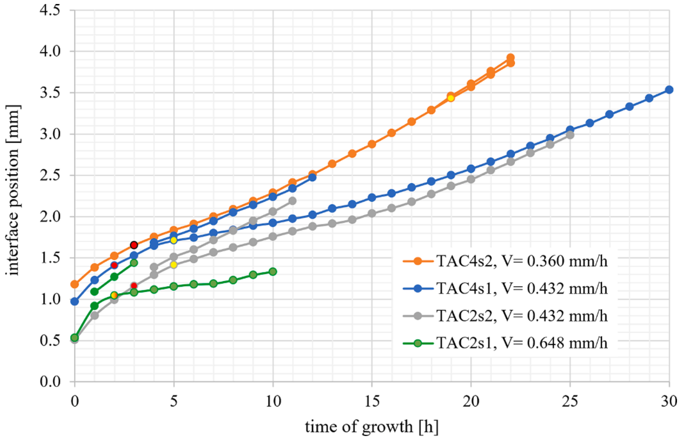

Fig. 4. Interface positions as function of time for four experiments that reveal a single-phase 2D layer at the top of the tilted interface. Taken are the interface positions at the front window. All curves bifurcate into two branches; one defined by the tip position of the advancing thin layer planar/cellular growth and a second indicating the position of the interface that is left behind (roots of the thin layers). These second branches terminate when the interface in the sample is fully cellular. The beginning of PCG for the bulk interface is indicated by the red dots. Instability of the leading thin solid layer is indicated by yellow dots. For TAC2s1 the red and yellow dots overlay.

between the frontmost thin solid layer and the left-behind PCG further increased with time, as shown in Fig. 4.

Note that TAC2s4 and TAC4s2 were processed with the same pulling velocity. For TAC2s4 planar PCG lasted around 9.5 h and ended with single-phase planar growth. Contrarily, PCG for TAC4s2 lasted the full processing period. After around 19 h of pulling, small single-phase cells occur at the top of the tilted interface while PCG is still ongoing [23]. That's why it is classified here as partly planar PCG. The small difference in segment concentration, $c_0 = 49.3 \pm 1$ mol% NPG for TAC2s4 and $c_0 = 50.2 \pm 1$ mol% NPG for TAC4s2, can not explain this different behavior. A severe difference between this two runs is the inclination of the interface; for TAC2s4 the inclination nearly vanished with time, whereas for TAC4s2 it increased slightly.

Obviously, the interface inclination is a severe factor that influences the further development of PCG. In the present experiments, for larger pulling velocities the initial interface inclination (caused by a thermal bias) leads to the formation of a thin solid layer at the front window of a cartridge. The tip of such a thin solid layer is located ahead of the bulk s/l interface. Therefore, diffusion can occur in the growth direction and sideways. The formation of such thin solid layers is promoted by the fact that a growing interface that is inclined against the cartridge axis possesses a concentration profile that is also inclined. The solute pileup ahead of the foremost part of such an inclined s/l interface is thus affected not only by diffusion in the longitudinal direction but also in the lateral direction. As a consequence, the foremost part of the inclined interface can grow faster than the rest of the interface. The opposite is true for the backmost part of an inclined s/l interface. Here, solute diffusion away from the interface is hindered by the presence of the containment boundary.

According to the initial interface temperature and the TRIS-NPG phase diagram, TAC2s2 has a composition that is out of the peritectic interval, namely $c_0 = 44.0 \pm 1$ mol% NPG. Therefore, only the pro-peritectic α-phase should solidify. However, the large inclination of the s/l interface led to a concentration increase at the backmost part of the interface, such that the β-phase could grew there. The same is true for segments TAC4s1 and TAC4s2. Therefore, it can be stated that for the partly planar/cellular PCG cases, β-phase bands grew in the gap along the rear window, where, owing to the inclined growth, the solute concentration was high. When the β-phase band reaches (coagulated or individually) the α/l interface PCG starts. This is the same mechanism for starting PCG as for the fully planar PCG cases.

Declaration of Competing Interest

The authors declare that they have no known competing financial interests or personal relationships that could have appeared to influence the work reported in this paper.

Acknowledgements

This research was supported by the European Space Agency (ESA) in the framework of the project METCOMP and by the Austrian Research Promotion Agency (FFG) under grant number 865969.

References

[1] H.W. Kerr, W. Kurz, Solidification of peritectic alloys, Int. Mater. Rev. 41 (1996) 129–164, https://doi.org/10.1179/095066096790151231.

[2] T.S. Lo, S. Dobler, M. Plapp, A. Karma, W. Kurz, Two-phase microstructure selection in peritectic solidification: from island banding to coupled growth, Acta Mater 51 (2003) 599–611, https://doi.org/10.1016/S1359-6454(02)00440-8.

[3] S. Dobler, T.S.S. Lo, M. Plapp, A. Karma, W. Kurz, Peritectic coupled growth, Acta Mater 52 (2004) 2795–2808, https://doi.org/10.1016/j.actamat.2004.02.026.

[4] W.J. Boettinger, The structure of directionally solidified two-phase *Sc*-Cd peritectic alloys, Met. Trans. 5 (1974) 2023–2031, https://doi.org/10.1007/BF02644495.

[5] R. Trivedi, Theory of Layered-Structure Formation in Peritectic Systems, Met. Mater. Trans. A. 26 (1995) 1583–1590, https://doi.org/10.1007/BF02647608.

[6] J.H. Lee, J.D. Verhoeven, Peritectic formation in the Ni-Al system, J. Cryst. Growth. 144 (1994) 353–366, https://doi.org/10.1016/0022-0248(94)90477-4.

[7] M. Vandyoussfi, Microstructure Selection during Directional Solidification and Solid-State Transformation in Ke-Ni Alloys, Ph.D. at Swiss Federal Institute of Technology, Lausanne, 1997.

[8] S. Dobler, W. Kurz, Phase and microstructure selection in peritectic alloys under high G-V ratio, Z. Met. 95 (2004) 592–595, https://doi.org/10.3139/146.017993.

[9] O. Hunziker, M. Vandyoussefi, W. Kurz, Phase and microstructure selection in peritectic alloys close to the limit of constitutional undercooling, Acta Mater 18 (1998) 6325–6336, https://doi.org/10.1016/S1359-6454(98)00336-X.

[10] A. Karma, W.J. Rappel, B.C. Fuh, R. Trivedi, Model of banding in diffusive and convective regimes during directional solidification of peritectic systems, Met. Mater. Trans. A. 29 (1998) 1457–1470, https://doi.org/10.1007/s11661-998-0361-1.

[11] P. Mazumder, R. Trivedi, A. Karma, Mechanisms of layer structure formation in peritectic alloys. ***MRS Fall Symp***. 1997, 1998, pp. 39–44, https://doi.org/10.1557/PROC-481-39.

[12] R. Trivedi, J.S. Park, Dynamics of microstructure formation in the two-phase region of peritectic systems, J. Cryst. Growth. 235 (2002) 572–588, https://doi.org/10.1016/S0022-0248(01)01803-6.

[13] T.A. Lograsso, B.C. Fuh, R. Trivedi, Phase selection during directional solidification of peritectic alloys, Met. Mater. Trans. A. 36 (2005) 1287–1300, https://doi.org/10.1007/s11661-005-0221-1.

[14] R. Trivedi, The role of heterogeneous nucleation on microstructure evolution in peritectic systems, Scr. Mater. 53 (2005) 47–52, https://doi.org/10.1016/j.scriptamat.2005.03.019.

[15] R. Trivedi, J.H. Shin, Modelling of microstructure evolution in peritectic systems, Mater. Sci. Eng. A. 414 (2005) 288–295, https://doi.org/10.1016/j.msea.2005.09.027.

[16] J. Valloton, J.D. Wagnière, M. Rappaz, Competition of the primary and peritectic phases in hypoperitectic Cu-Sn alloys solidified at low speed in a diffusive regime, Acta Mater 60 (2012) 3840–3848, https://doi.org/10.1016/j.actamat.2012.03.030.

[17] J. Valloton, J.A. Dantzig, M. Plapp, M. Rappaz, Modeling of peritectic coupled growth in Cu-Sn alloys, Acta Mater 61 (2013) 5549–5560, https://doi.org/10.1016/j.actamat.2013.05.011.

[18] J.S. Park, R. Trivedi, Convection-induced novel oscillating microstructure formation in peritectic systems, J. Cryst. Growth. 187 (1998) 511–515, https://doi.org/10.1016/S0022-0248(97)00884-1.

[19] P. Mazumder, R. Trivedi, A. Karma, A model of convection-induced oscillatory structure formation in peritectic alloys, Met. Mater. Trans. A. 31 (2000) 1233–1246, https://doi.org/10.1007/s11661-000-0119-x.

[20] S. Liu, R. Trivedi, Effect of thermosolutal convection on microstructure formation in the Pb-Bi peritectic system, Met. Trans. A. 37 (2006) 3293–3304, https://doi.org/10.1007/BF02586164.

[21] J. Mogeritsch, W. Sillekens, A. Ludwig, In-situ observation of coupled growth morphologies in organic peritectics under pure diffusion conditions, TMS Annu. Meet. Symp. "Mater. Res. Microgr. (2022) 1429–1441, https://doi.org/10.1007/978-3-030-92381-5_136.

[22] A. Ludwig, J.P. Mogeritsch, Observation of peritectic couple growth for a hyper-peritectic alloy under microgravity conditions, IOP Conf. Ser. Mater. Sci. Eng. 1274 (2023), 012032, https://doi.org/10.1088/1757-899X/1274/1/012032.

[23] A. Ludwig, J.P. Mogeritsch, *In-situ* study of peritectic couple growth under purely diffusive conditions, Met. Mater. Trans. A. (2023), https://doi.org/10.1007/s11661-023-07052-6 published online: 26. April.

[24] A. Ludwig, J. Mogeritsch, M. Kolbe, G. Zimmermann, L. Sturz, N. Bergeon, B. Billia, G. Faivre, S. Akamatsu, S. Bottin-Rousseau, D. Voss, Advanced solidification studies on transparent alloy systems: a new european solidification insert for Material Science Glovebox on board the International Space Station, JOM 64 (2012) 1097–1101, https://doi.org/10.1007/s11837-012-0403-4.

[25] L. Sturz, M. Schraml, P. Möckel, W. Köhler, V.T. Witusiewicz, G. Zimmermann, Influence of Soret effect on the pre-solidification state in the neopentylglycol-(D) camphor system during microgravity experiments, J. Cryst. Growth. 601 (2023), 126953, https://doi.org/10.1016/j.jcrysgro.2022.126953.

[26] W.G. Pfann, Temperature gradient zone melting, AIME 203 (1955) 961–964, https://doi.org/10.1007/BF03377594.

[27] W.A. Tiller, Migration of a liquid zone through a solid, J. Appl. Phys. 34 (1963) 2757–2769, https://doi.org/10.1063/1.1729806.